The middle ear of the pink fairy armadillo *Chlamyphorus truncatus* (Xenarthra, Cingulata, Chlamyphoridae): comparison with armadillo relatives using computed tomography

Ana P. Basso[1,2], Nora S. Sidorkewicj[1,2], Emma B. Casanave[2,3], Matthew J. Mason[4]

[1]*Departamento de Biología, Bioquímica y Farmacia, Cátedra de Anatomía Comparada, Universidad Nacional del Sur (UNS), Bahía Blanca, Argentina*

[2]*Instituto de Investigaciones Biológicas y Biomédicas del Sur (INBIOSUR), UNS y Consejo Nacional de Investigaciones Científicas y Técnicas (CONICET), Bahía Blanca, Argentina*

[3]*Departamento de Biología, Bioquímica y Farmacia, Cátedra de Fisiología Animal, UNS, Bahía Blanca, Argentina*

[4]*Department of Physiology, Development & Neuroscience, University of Cambridge, Cambridge, UK*

Abstract

The pink fairy armadillo *Chlamyphorus truncatus* is the smallest extant armadillo and one of the least-known fossorial mammals. The aim of this study was to establish if its middle ear is specially adapted to the subterranean environment, through comparison with more epigeic relatives of the groups Euphractinae (*Chaetophractus villosus*, *Chaetophractus vellerosus*, *Zaedyus pichiy*) and Dasypodinae (*Dasypus hybridus*). We examined the middle ears using micro-computed tomography and subsequent 3D reconstructions. *Dasypus hybridus* has a relatively small middle ear cavity, an incomplete bulla and 'ancestral' ossicular morphology.

The other species, including *Chlamyphorus*, have fully ossified bullae and middle ear ossicles with a morphology between 'transitional' and 'freely mobile', but in all armadillos the malleus retains a long anterior process. Unusual features of armadillo ears include the lack of a pedicellate lenticular apophysis and the presence, in some species, of an element of Paaw within the stapedius muscle. In common with many subterranean mammals, *Chlamyphorus* has a relatively flattened malleo-incudal articulation and appears to lack a functional tensor tympani muscle. Its middle ear cavity is not unusually enlarged, and its middle ear ossicles seem less robust than those of the other armadillos studied. In comparison with the euphractines, there is no reason to believe that the middle ear of this species is specially adapted to the subterranean environment; some aspects may even be indicative of degeneration. The screaming hairy armadillo, *C. vellerosus*, has the most voluminous middle ear in both relative and absolute terms. Its hypertrophied middle ear cavity likely represents an adaptation to low-frequency hearing in arid rather than subterranean conditions.

Key words: armadillos, middle ear; subterranean; morphology; lenticular apophysis.

Introduction

The Xenarthra comprise an ancient group of South American mammals, the most successful of the placental assemblages that dispersed to the north during the Great American Biotic Interchange of the late Tertiary (McDonald, 2005). Despite their great diversity in the past, there are relatively few extant armadillos, sloths and anteaters. These animals are widely distributed in South and Central America with a single species, the nine-banded armadillo (*Dasypus novemcinctus*), reaching southern North America. The position and phylogenetic relationships of Xenarthra are controversial and under constant revision: at present they are considered as one of the four major clades of placental mammals (Madsen et al. 2001; Murphy et al. 2001) and the sister group of Afrotheria within Atlantogenata (Tarver et al. 2016).

Armadillos (Cingulata) are the most speciose xenarthrans today. Based on molecular phylogenetic analyses, Gibb et al. (2016) proposed assigning all the extant species to two distinct families, Dasypodidae and Chlamyphoridae. The former contains only one subfamily (Dasypodinae), represented by the single genus *Dasypus* (long-nosed armadillos). The latter includes eight genera grouped into three subfamilies: Chlamyphorinae (fairy armadillos), Euphractinae (hairy armadillos) and Tolypeutinae (giant, three-banded and naked-tailed armadillos). Delsuc et al. (2012) proposed that the fossorial lifestyle of fairy armadillos probably evolved as a response to the Oligocene aridification that occurred in South America, after their divergence from the Tolypeutinae around 32 million years ago.

The possession of a flexible carapace formed by dermal bones is not the only bizarre characteristic of armadillos. Other peculiarities are homodonty, absence of enamel in adults, dental aberrancies (Sidorkewicj & Casanave, 2013), a striking plasticity of some of their organ systems (Casanave & Galíndez, 2008), an obligate monozygotic polyembryony in *Dasypus* (Loughry et al. 1998) and relatively low metabolic rates (McNab, 1980). Almost all members of the group will burrow to some extent, although they differ in their digging habits (Milne et al. 2009; Galliari, 2014). Vizcaíno et al. (1999) classified armadillos into three categories, later modified by Milne et al. (2009): (a) non-diggers (mainly cursorial species: *Tolypeutes*), (b) generalised diggers (Dasypodinae and Euphractinae) and (c) specialised diggers (giant armadillo *Priodontes maximus*, naked-tailed armadillos of the genus *Cabassous*, and the chlamyphorines *Chlamyphorus truncatus* and *Calyptophractus retusus*).

The pink fairy armadillo *C. truncatus*, known also as pichiciego menor or pichiciego pampeano, is the smallest extant armadillo. It is usually considered a strictly subterranean species (see e.g. Borghi et al. 2011; Delsuc et al. 2012; Torres et al. 2015), but it lacks the extreme anatomical adaptations to a subterranean environment found in e.g. some talpid moles, mole-rats and golden moles. Although it feeds mainly underground, it also consumes above-ground items (Meritt, 1985) and is said to leave its burrows occasionally (Minoprio,

1945; Rood, 1970). A more appropriate term for *C. truncatus* might be 'fossorial' as defined by Lange et al. (2004), i.e. having habits intermediate between generalized epigeic and strictly subterranean forms. *Chlamyphorus* is endemic to central Argentina (Wetzel et al. 2007), where it inhabits sandy plains, dunes, and scrubland. Categorised as a sand-swimmer by Borghi et al. (2002), it is rarely seen due to its nocturnal and subterranean habits, and this makes its study particularly difficult. Although it has been generally accepted that this species has declined in distribution and abundance in recent years (Superina, 2006; Aguiar & Fonseca, 2008; Ojeda et al. 2012), Borghi et al. (2011) found that populations persist along most of their original range and added new records outside the historical distribution map. However, there is an almost total lack of biological data on this species, one reason why it is currently listed as Data Deficient in the IUCN Red List of Threatened Species (Superina et al. 2014). There is an urgent need to fill gaps in our knowledge of these enigmatic creatures.

The hearing of subterranean and fossorial mammals has attracted considerable interest owing to the unusual acoustic environment underground. Several studies have identified common middle ear features in species inhabiting underground ecotopes (e.g. Burda et al. 1989, 1992; Mason, 2001, 2013; Begall & Burda, 2006). The malleo-incudal complex typically has a 'freely mobile' morphology, to use Fleischer's (1978) terminology, characterised by ossicles with relatively large heads, a manubrium of the malleus roughly perpendicular to the 'anatomical axis' extending between anterior process of the malleus and short process of the incus, and relatively loose attachments of these two ossicular processes with the skull. Other characteristics commonly found among subterranean mammals are reduced or absent middle ear muscles, stapedial arteries (where present) contained within bony tubes, tympanic membranes without a *pars flaccida* and relatively large stapes footplates (Burda et al. 1992; Mason, 2001, 2003, 2004, 2013, 2015; Begall & Burda, 2006; Begall et al. 2007; Mason et al. 2010, 2016). Low-frequency sounds have been found to propagate better than higher frequencies in subterranean tunnels (Heth et al. 1986), and it has duly been suggested that at

least some of these 'subterranean' ear characteristics improve the transmission of low-frequency sound to the cochlea (Burda et al. 1989, 1992). However, the most obvious anatomical feature that one would expect in a 'low-frequency' middle ear would be a capacious cavity, serving to increase acoustic compliance (Mason, 2016a). Those subterranean mammals which have been investigated so far do not have significantly larger middle ear cavities than non-fossorial taxa (Mason, 2001). Accordingly, behavioural audiograms from subterranean rodents show that, while they tend to have hearing restricted to low frequencies, it is not unusually acute at those frequencies (Heffner & Heffner, 1990, 1992, 1993; Brückmann & Burda, 1997; Gerhardt et al. 2017).

In order to assess whether ear structures in subterranean species represent true adaptations towards hearing underground, they must be compared with those of close, terrestrial relatives. Among talpid moles (Eulipotyphla; Talpidae), 'subterranean' middle ear characteristics are found in the more exclusively subterranean species, and are clearly derived in comparison with e.g. shrews and shrew-moles (Mason, 2006). The middle ears of spalacid mole-rats (Rodentia; Spalacidae) also seem to be derived in comparison with those of terrestrial muroid rodents (Mason et al. 2010). In other subterranean rodents such as bathyergid mole-rats, *Ctenomys* and *Spalacopus*, however, similar anatomical features of the middle ear appear to be retained, primitive characteristics of the Ctenohystrica group to which these animals belong (Mason, 2004, 2016a; Begall & Burda, 2006; Argyle & Mason, 2008).

There is only limited information available regarding the middle ear anatomy of the pink fairy armadillo (Hyrtl, 1845; Roig, 1972; Fleischer, 1973; Segall, 1976; Patterson et al. 1989, 1992). Segall (1976) concluded that the ear of *Chlamyphorus* is "influenced by its fossorial life", but a comprehensive, comparative account is lacking. We present the first micro-CT reconstructions of the middle ear of *C. truncatus*, and compare these with those of more epigeic armadillos of the groups Euphractinae and Dasypodinae, coming from the same

geographical area. The purpose was to establish if the middle ear of *C. truncatus* does indeed show signs of being specially adapted to the subterranean environment.

Materials and methods

Preparation of samples

Thirteeen skulls of adult armadillos belonging to the collection of the Cátedra de Anatomía Comparada and INBIOSUR-CONICET (UNS) were used. Species were *Chlamyphorus truncatus* (pink fairy armadillo; n =3), *Chaetophractus villosus* (large hairy armadillo; n = 4), *Chaetophractus vellerosus* (screaming hairy armadillo; n = 1), *Zaedyus pichiy* (pichi; n = 3) and *Dasypus hybridus* (southern long-nosed armadillo; n = 2). All animals came from the province of Buenos Aires, Argentina. The specimens of *C. truncatus* had been deposited in the collection prior to the study, and originated from private donations. The other material came from animals found dead but with the skulls in good condition; they were collected by permission of the Ministry of Agroindustria of the Province of Buenos Aires, Flora and Fauna Division (Regulation N° 77, 28/09/2017; Exp. 22500-41961/17). Specimen data are presented in Table 1.

After removal, the heads were preserved frozen until use. They were then defrosted and subjected to repeated boiling periods (15-20 minutes each) within a mixture of water and biological laundry detergent, until the muscles detached from the bone. Between boiling periods, the bone was allowed to dry completely and the cleaning was continued with the help of dissection implements. Although the external soft tissues of the skull were largely removed by this cleaning procedure, the middle ear muscles were allowed to dry *in situ* together with, in *Dasypus*, some of the material holding the ectotympanic in place. Total skull length (TSL, anterior edge of the premaxilla to the most posterior point of the nuchal crest) was measured

in the cleaned skulls by means of digital callipers (0.01 mm); measurements are presented in Table 1.

Micro-computed tomography and reconstruction

Micro-CT scans were made of intact skulls of two specimens of *Z. pichiy*, but one specimen of each of the other species considered. To give enhanced detail of the middle ear structures, scans were also made of the posterior skull only, and in some cases dissected-out temporal regions, each of which included one auditory bulla (Table 1). Samples were placed on radiotranslucent material to prevent movements during scanning. Scans were made using a Nikon XT H 225 micro-CT scanner. The settings used were 125-130 kV and 120-130 µA. The images were reconstructed from 1080 projections, each with an exposure time of 1000 ms and two frames averaged per projection. CT AGENT XT 3.1.9 and CT PRO 3D XT 3.1.9 (Nikon Metrology, 2004-2013) were used to process the scan data. Cubic voxel side-lengths were 13.8-50.9 µm (see supplementary table S1 for scan details).

To facilitate image processing, exported 16-bit tiff files were converted to 8-bit jpg files using Adobe Photoshop CS 8.0 (Adobe Systems Inc. 2003). Most of the 3D reconstructions were made using Stradwin 5.4 (Graham Treece, Andrew Gee & Richard Prager, 2018). Within this program, the boundaries of structures of interest were identified and outlined in order to create the reconstructions. The outlining of ossicles involved automated thresholding followed by manual correction, but where boundaries were less distinct all outlining had to be performed manually. For larger structures such as cavities, structures were outlined in a subset of the available tomograms, the software interpolating in-between. For smaller structures such as ossicles, a higher proportion of the available tomograms was used. Reconstructions of the whole skulls and tympanic rings were made using MicroView 2.5.0 (Parallax Innovations Inc., 2019). Images of right or left ears were laterally inverted where necessary, to facilitate comparison in the composite figures.

176

177 **Morphofunctional parameters**

178 The parameters measured from the 3D reconstructions were volumes of the middle ear
179 cavities and ossicles, lever arms of the malleus and incus, and areas of the tympanic
180 membrane and of the stapedial footplate. Although all CT scans were examined,
181 measurements of middle ear structures were made only from the higher-resolution scans of
182 the temporal bones or posterior skulls. If both ears had been scanned, right-side
183 measurements only were recorded unless that ear was damaged.

184 The volumes of the tympanic cavity and associated subcavities were calculated from
185 reconstructions of their boundaries. The position of the tympanic membrane, which forms part
186 of the boundary of the tympanic cavity, was in each case estimated from the positions of the
187 bony tympanic annulus and the manubrium mallei. In order to calculate air-space volumes,
188 middle ear ossicle and muscle volumes were subtracted from the overall cavity volumes.
189 Because there is no very clear demarcation between the confluent tympanic cavity and
190 epitympanic recess, the division that was made between them was somewhat arbitrary. As
191 such, their relative volumes must be considered as approximations only.

192 The line between anterior process of the malleus and short process of the incus has been
193 referred to as the 'anatomical axis' (Lavender et al., 2011), used as an estimate of where the
194 ossicular rotatory axis might be, at low frequencies. Because the anterior process is very long
195 in armadillos and in articulation with the skull along most of this length, the thin, proximal part
196 of the process, where it meets the transversal lamina, was considered to be the most likely
197 point of flexibility about which the ossicles would rotate. Stradwin was therefore used to
198 obtain the spatial coordinates (x, y, z) of a point in this position on the anterior process (A),
199 and another at the short process of the incus. These were used to calculate the equation of the
200 line joining both points. The coordinates of a point at the tip of the manubrium (B) were also
201 obtained. To calculate the malleus lever arm (ML) two vectors were considered, *w* with origin

in A and end in B, and the vector v extending along the anatomical axis with the same origin as w. The orthogonal projection of w on v was

$$|w|\cos\alpha = \frac{\langle w,v\rangle}{|v|},$$

where $\langle w,v\rangle$ is the scalar product between vectors, $|w|$ and $|v|$ are the moduli of vectors w and v respectively, and α is the angle between them. Then the distance from the rotatory axis to the point B, which represents ML, was calculated as:

$$\left|\frac{\langle w,v\rangle}{|v|}\frac{v}{|v|} - w\right|$$

The same procedure was used to obtain the incus lever arm (IL), as the perpendicular distance from the anatomical axis to the centre of the incudal articulation facet for the stapes. The anatomical lever ratio (LR) was then calculated as ML/IL. All calculations were programmed using Excel.

The tympanic membrane area (TA) was obtained from the MicroView reconstructions of the bony tympanic ring. Each reconstruction was oriented in MicroView such that the perimeter of the tympanic ring was in the plane of the computer screen, and then the 2D image (screenshot) was exported to ImageJ 1.52e (National Institutes of Health, USA). Using the automated measure function of the software and an appropriate scaling factor, the area of the tympanic membrane was estimated as a flat surface. The same procedure was used to estimate the stapedial footplate area (FA), from the medial view of the reconstructed footplate. The anatomical area ratio AR was then calculated as TA/FA.

To enable fairer comparisons among species, the parameters were considered relative to the total skull length (TSL), used as an index of cranial size. Body mass was not used because, besides being subject to high intraspecific variation depending on sex, age, nutritional and health status, etc., individual values were not available for our specimens. To take into account the allometric scaling of middle ear structures expected among mammals (Nummela, 1995; Mason, 2001), least-squares linear regressions were performed for the relationship of each

parameter with TSL on log-transformed data. Deviations of the slope coefficient *b* from the theoretical value of isometric growth (*b* = 3, 2 or 1 for volumes, areas and linear measurements against TSL, respectively) were examined by t-test using Excel. Since no relationship is expected between a ratio and skull length, the area and lever ratios of all the species were directly compared. This simple approach has obvious shortcomings: the sample size was small, the numbers of specimens of each species unequal and the relationships between species were not taken into account. For these reasons, the regression relationships were used only to identify species which clearly have relatively large or small ear structures, in comparison with the general trend.

Results

A detailed description of the external bullar anatomy of the Cingulata is found in Patterson et al. (1989). Therefore, we will only briefly mention the morphological characteristics of the bulla, concentrating instead on the ossicles and other internal features that are significant from a functional point of view.

The middle ear of *Chlamyphorus truncatus*

The auditory bulla is completely ossified, well developed, markedly swollen and clearly demarcated from the basicranium (Fig. 1). It is roughly ovoid in ventral view and its long axis is oriented approximately 45 degrees relative to the sagittal plane of the skull. It was not possible to distinguish the boundaries between its component bones in our adult specimens. The tympanic membrane is supported by a complete, bony tympanic ring (Fig. 2D). The bony rim is almost circular except for a rounded embayment in the epitympanic region, just dorsal to the lateral process of the malleus. This notch, which may hold a *pars flaccida*, represented on average 8% of the total area of the membrane contained within the rim (Table 3). The lateral part of the bulla contains the recessus meatus, which abruptly narrows to form the external

opening without the interposition of a bony tube. The bullar walls are not pneumatised (Fig. 3A).

Medial to the tympanic ring, the middle ear cavity is divided into two widely-communicating subcavities: a large tympanic cavity and a smaller epitympanic recess (Figs 3A and 4A; Table 2). The latter, which represents 13% of the total middle ear cavity volume, houses the articulated malleus head and incudal body. It is closed laterally by a bony wall. The epitympanic recess is irregularly shaped and obliquely directed from dorsolateral to ventromedial. Below this, the cochlear promontory protrudes into the tympanic cavity, elongated in the rostrocaudal direction. The oval window is caudodorsal to the promontory and the round window caudal, the two separated by a narrow bridge of bone.

The middle ear ossicles are formed entirely from compact bone. The malleus and incus were not fused together, the articulation being easily distinguishable from a medial view of the ossicular reconstructions as a slightly sinuous line (Fig. 5A). The malleus head is small and essentially hemispherical, with a slight mediolateral compression. Its articular surface is oval in shape from a posterior view and relatively shallow, the dorsomedial and ventrolateral facets not being clearly divided from each other. The anterior process is long and narrow. It curves ventrally, expanding slightly as it does so, and is fused to the ectotympanic only at the tip, with most of the process being attached only by soft tissue to the surrounding skull. There is a conspicuous perforation between the malleus head, which is excavated rostrally, and the base of the anterior process, perhaps for the passage of the chorda tympani nerve. The head continues in a short neck that retains the mediolateral compression in its first half, but then twists so that its terminal half is flattened rostrocaudally. In one of the two specimens (UNSCTMA1), we observed what could represent a markedly reduced transversal lamina between the neck and the anterior process. The manubrium is moderately long and forms an approximately 60° angle with the anatomical axis. The lateral process is rounded and not prominent, developing into a narrow margin inserting into the tympanic membrane. This

inserting margin is somewhat irregularly shaped. The proximal part of the manubrium has a marked rostrocaudal compression where it becomes very thin. Although a strand of soft tissue was found to cross the middle ear cavity to insert on the manubrium of the malleus in the appropriate position, no trace of a tensor tympani muscle belly could be identified, and there is no muscular process on the malleus.

The incus body is wide in dorsoventral direction, defining a triangular shape that has a mediolateral compression similar to that of the malleus head (Fig. 5A). The short process is sturdy and conical. The long process is wide and turns slightly medially, ending at the level of the proximal third of the manubrium. It becomes thin and spatulate distally, directly forming the articulation surface with the stapes head. The incudo-stapedial joint is therefore based on a simple contact between the flattened terminal end of the long process and the head of the stapes, without an intervening lenticular apophysis (Fig. 6A).

The stapes is typically bicrurate (Fig. 5A). The oval head narrows to form a long and flattened neck region. This neck appears perforated in one ear of UNSCTSI1 (Fig. 5A, 6A) and is broken on one side of UNSCTMA1, attesting to how thin the bone is here. There is a well-developed muscular process; a stapedius muscle was identifiable from the CT scans but no element of Paaw was visible within it. Between neck and footplate, the stapedial crura diverge to surround a sizeable intercrural foramen, but no artery passes through this. Both stapedial crura are made of flat, thin bone, lacking internal sulci. The anterior crus is wider than the posterior one. The insertions of the crura leave around a quarter of the footplate free on each side. The flattened vestibular surface of the footplate resembles the sole of a shoe in general shape, wider caudally (Fig. 6A). It is made of thin bone, with only very slight thickening around its edge.

The middle ears in euphractine armadillos

The limits of the auditory bullae of the euphractine species (*Chaetophractus villosus*, *Chaetophractus vellerosus* and *Zaedyus pichiy*) with respect to the basicranium are more irregular and less clear than in *Chlamyphorus*. These three taxa are characterised by a lateral extension of the bulla into a long, bony external auditory meatus, extending dorsolaterally from the recessus meatus (Figs 1 and 3B, C, E). The tympanic rings are approximately circular in these species (Fig. 2A, B, C). The single adult specimen of *C. vellerosus* had no epitympanic notch at all. The specimens of *Z. pichiy* had visible sutures where the two limbs of the ectotympanic bone converged dorsally, but there was little if any notch in this position. *Chaetophractus villosus* had a larger epitympanic notch, but not as prominent as in *Chlamyphorus*. The entotympanic bones of *C. villosus* and *Z. pichiy,* which contribute to the medial walls of the bullae, have internal cavities that are somewhat larger in the latter, but these do not represent pneumatisations from the middle ear cavity and are presumably marrow spaces (Figs 3B, E).

In *C. villosus* and *Z. pichiy*, the structure of the middle ear cavity is simple and, as in the pink fairy armadillo, it can be divided into tympanic cavity and epitympanic recess (Figs 3 and 4, B and E). Relative to the total middle ear volume, the epitympanic recesses in these animals are similar in size to what was found in *C. truncatus*, representing on average 18% (*C. villosus*) and 20% (*Z. pichiy*) of the total cavity volume. In *C. vellerosus*, there are marked differences in the structure and size of the middle ear cavity (Figs 3C and D; Fig. 4C). Although it is a species of comparable body mass and skull size to *Z. pichiy* (Table 1), its middle ear cavity volume is on average more than four times larger. The epitympanic recess is markedly expanded dorsally, representing 41% of the total middle ear cavity volume (Table 2). Although there are low ridges projecting from its walls, it essentially represents one large cavity. Between the epitympanic recess and the tympanic cavity, just caudal to the incus, there is a largely separate compartment interpreted as a mastoid cavity, which represents 9% of the total middle ear

cavity volume (Table 2 and Fig. 4C). Despite the great development of the middle ear cavity in this species, there is no contact between left and right cavities in the sagittal plane of the skull.

The middle ear ossicles of these euphractine armadillos have the same general characteristics as in the pink fairy armadillo, although some differences were observed (Figs 5B, C and D). The malleo-incudal articulations are less flattened, the articulation facets on malleus and incus being more sharply demarcated from each other. The mallei differ in head shape: more robust and prominent rostrally in *Chaetophractus* species than in *Chlamyphorus*, intermediate in *Z. pichiy*. Small transversal laminae are present in the three taxa, this structure being least developed in *C. vellerosus* (Fig. 5C). The lateral processes were more prominent in these species than in *Chlamyphorus*. Even though there were no distinct muscular processes, only very slight thickenings at the bases of the manubria, the scans revealed the presence of a tensor tympani muscle inserting on the malleus in at least one specimen of every species. In *C. vellerosus* and *Z. pichiy* there is only a limited area of synostosis between the distal part of the anterior process and the ectotympanic, as in *Chlamyphorus*. In *C. villosus* there is no fusion at all and the connection seems to occur entirely through fibrous tissue; this may account for the ease with which the malleus is dislodged and found loose inside the bulla in clean skulls of this species (APB: pers. obs.). The incus is similar in the three euphractines, although in both *Chaetophractus* species the long processes bend a little more medially. There was no lenticular apophysis in any species (Fig. 6B, C and D). The stapedes, although having the same basic bicrurate morphology, differ in the robustness of their crura, resulting in intercrural foramina of different relative sizes (biggest in *C. villosus*, smallest in *Z. pichiy*: Fig. 4). These differences account, at least partly, for the interspecific variation in the relative volumes of the stapedes (see below).

A stapedius muscle was identified in at least one specimen of each species. A small, bony element of Paaw was present within the stapedius muscle of *C. vellerosus* (Fig. 4D) and some

specimens of *C. villosus* (UNSCVIHA83, one side only, and UNSCVIMA91), but it was never in direct contact with the stapes. No trace of an element of Paaw was detected in *Z. pichiy*.

The middle ear of *Dasypus*

The dasypodine armadillo *Dasypus hybridus* has a middle ear conformation that is quite different from those of the other species studied (Fig. 1). The ectotympanic bone forms an incomplete ring, attached to the rest of the skull only by soft tissues (Figs 2E and 3F), which means that there is no complete, bony auditory bulla and no development of a bony external auditory meatus. We did not find cartilage in the ventral wall of the tympanic cavity but several isolated bony fragments were found between ectotympanic and cochlear promontory in both specimens examined, bilaterally, which could correspond to entotympanic elements (Figs 1 and 3F). Because the ectotympanic crura do not closely converge and there was no bony lateral wall to the epitympanic recess, it was impossible to ascertain the boundaries of any *pars flaccida*. The tympanic membrane area enclosed within the ectotympanic, which is expected to comprise the *pars tensa* alone, is similar to that of the much smaller *C. truncatus* (Table 3).

Although the middle ear cavity walls in *Dasypus* are partially composed of soft tissue, this had dried in place and could be discerned in the CT scans, allowing us to measure the cavity volume. The components of the middle ear cavity are comparable in absolute volume with those of the pink fairy armadillo (Table 2; Figs 3F and 4F). The contributions of the tympanic cavity and epitympanic recess to the total middle ear cavity volume were 82% and 18%, respectively, markedly different from what was observed in *C. vellerosus* but similar to the other species (Table 2).

The malleus and incus are both substantially different from those of the other taxa (Fig. 5E). The malleus head is small, and its articular surface takes the form of a deep notch. The two facets meet at an acute angle. A long and stout anterior process is present, which expands

distally but is not synostosed to the closely adjacent ectotympanic bone. From the base of the anterior process and ventral head emerges a substantial transversal lamina, which thickens ventrally towards the base of the manubrium, but there is no clear prominence here which could be regarded as an orbicular apophysis. The manubrium is oriented almost parallel to the anatomical axis, and it has no lateral process. Although there is no distinct muscular process, a large, fleshy tensor tympani could be seen in the scans inserting on the thickened part of the malleus near the base of the manubrium. The incus is relatively small with respect to the malleus (Table 3). The short process is relatively longer and thinner than in the other armadillos; its tip ends closer to the skull than in the other species, suggesting that the ligament anchoring it to the periotic is short and stubby. The long process is approximately perpendicular to the anatomical axis, and as in the other armadillos there is no lenticular apophysis. The stapes appears rotated relative to the long process (Fig. 6E). The stapes head is oval and continues into a neck that is relatively shorter than those of the other species (Fig. 5E). Both crura are long, almost equally wide all along and inserted near the border of the footplate; they delimit a triangular intercrural foramen. The footplate is oval and relatively thick. The stapedial muscle is well-developed and a large element of Paaw, almost as long as the footplate and nearly in contact with the stapes, was clearly visible (Fig. 4F).

Comparative morphometry

All the regression relationships between the middle ear measurements and the skull size of the species examined were found significant except for the stapedial measurements and the malleus lever arm (Table 4). Although the slopes of the regression lines were positive, their values were below what would be expected from isometry in the cases of the stapes volume and stapes footplate area (Table 4), indicating that in the larger species those structures are relatively smaller than in the smaller species. Whereas points representing *C. truncatus*, *Z.*

pichiy and *C. villosus* were located on or close to the regression lines for all the parameters, *C. vellerosus* and *D. hybridus* systematically fell above and below the line, respectively (Fig. 7).

Area ratios varied considerably among species (Table 3). The lowest values were those of *C. truncatus* and *D. hybridus*, the highest those of *C. villosus*. Both *pars tensa* and stapes footplate areas were considerably larger in absolute terms in *C. vellerosus* than in *Z. pichiy* (Table 3), although these armadillos have similarly-sized skulls. The relatively long malleus lever arm of *C. vellerosus* gave it the highest lever ratio (Table 3).

Discussion

Our findings regarding the morphology of the middle ear of *C. truncatus* and its relatives are broadly in agreement with previous descriptions in the literature (Doran, 1878; Fleischer, 1973; Segall, 1976; Novacek & Wyss, 1986; Patterson et al. 1989, 1992; Sidorkewicj & Casanave, 2012). We begin by comparing our results to these published descriptions.

Segall (1976) described a long, bony tube in *Chlamyphorus* which formed part of the external ear canal, composed of two successive segments joined by fibrous tissue. From his description, this tube would appear to be the result of ossification of the normally cartilaginous parts of the external auditory meatus. We did not find any such ossified tube extending from the recessus meatus in any of our *Chlamyphorus* skulls. Segall's illustrations of the malleus show an ossicle completely lacking an anterior process, which he described as 'short', but our CT scans revealed the presence of a long anterior process, as noted by Fleischer (1973). Detachment of the malleus from the ectotympanic in armadillos usually involves the breakage of the anterior process (see also Sidorkewicj & Casanave, 2012; pers. obs.). This process, which is very narrow proximally in *Chlamyphorus*, had presumably snapped in Segall's specimen. This likely also accounts for the relatively abbreviated processes illustrated for other armadillos by Patterson et al. (1992). We found a structure that could represent a markedly reduced transversal lamina only in one specimen of *Chlamyphorus*;

Segall reported the presence of a small one, but this is largely a matter of interpretation of the nature of the structures at the junction of head, neck and anterior process.

The incus of *Chlamyphorus* was described and illustrated by Segall (1976) as having a finger-like posterior crus (short process in the present paper), but our specimens had a conical short process. He did not mention the unusual nature of the incudo-stapedial articulation, discussed later. He describes the stapes of *Chlamyphorus* as "of sauropsidan type, i.e. somewhat columellar", perhaps referring to the long, flattened stapedial neck. Fleischer (1973) suggested that a secondary columellar morphology could arise in mammals from the crura inserting towards the middle of the footplate, rather than at its periphery. It is important, however, to distinguish the morphology of the armadillo stapedes, which have relatively wide intercrural foramina, from the imperforated or micro-perforated stapedes found in sloths and the pygmy anteater *Cyclopes* (Doran, 1878; Novacek & Wyss, 1986; Patterson et al. 1992), which are more appropriately referred to as 'columellar'. An imperforate stapes with very thin neck is also found in the adult naked mole-rat *Heterocephalus glaber* (Mason et al., 2016).

Although some connective tissue strands were visible in the CT scans which might have represented vestiges, it seems that the tensor tympani muscle in *C. truncatus* is significantly reduced or absent. This has not previously been noted in this species. Although this represents an unusual feature among mammals in general, one of the middle ear muscles is commonly reduced or absent in subterranean species (Burda et al. 1992; Mason, 2001, 2013). The stapedius muscle was universally present in our armadillo specimens, and an element of Paaw was identified within it in at least one ear of our specimens of *Dasypus* and both *Chaetophractus* species, between muscle belly and tendon. This structure, first mentioned by Paaw (1615) in adult oxen, has frequently been mistaken for the lenticular apophysis of the incus (Graboyes et al. 2011). It has been decribed in species of bats, opossums, tree shrews, primates, carnivores, rodents and edentates (McClain, 1939; Henson, 1961; Hinchcliffe & Pye, 1969; Pye, 1972; Wible, 2009). Among armadillos, it has been previously described in *Dasypus*

novemcinctus (Reinbach, 1952; Wible, 2010). Henson (1961) suggested that the element of Paaw might function to reduce friction between the stapedius tendon and the middle ear mucosa. This hypothesis is questionable, given that the element of Paaw is lacking in many mammalian groups. The intraspecific variability that has been documented previously (Hinchcliffe & Pye, 1969) and was also found in the present study suggests that the element of Paaw has no vital function.

Finally, Sidorkewicj & Casanave (2012) found a small *pars flaccida* in the Euphractinae. This membrane could not be seen directly in the prepared skulls examined. It seems likely that *Dasypus* has relatively the largest *pars flaccida* among the species studied, sealing the epitympanic recess lateral to the bodies of malleus and incus. In the other species, its area could be more precisely estimated from dorsal embayments in the bony tympanic rim. This notch was smaller in *C. villosus* than in *Chlamyphorus*, insignificant in *Zaedyus* and absent in *C. vellerosus*. The *pars flaccida* (Shrapnell's membrane) is thought to be an ancestral feature among marsupial and placental mammals (Fleischer, 1978). Although it is present in some mammals known or suspected to have excellent low-frequency hearing, including gerbils, jerboas and sengis (Lay, 1972; Mason, 2013), it is very small or absent in most subterranean mammals (Burda et al., 1992; Mason, 2006). The fossorial armadillo *Chlamyphorus* would therefore appear to be unusual in this respect.

Evolutionary and functional implications

Although *Dasypus* is second only to *C. villosus* in size among the armadillos studied (Table 1), it has middle ear structures similar in size to those of *C. truncatus*, and in some cases smaller (Tables 2 and 3). Its middle ear shows a number of features likely to be ancestral for therians as a whole (Fleischer, 1978). These include the ectotympanic bone taking the form of an open ring which is only loosely connected to the skull by connective tissue. Novacek (1977) described for adult *Dasypus* the existence of a "cartilaginous cover of the ventral opening of

483 the tympanic chamber", which is rare among living mammals and was considered likely to
484 represent a specialised condition. Small cartilaginous elements were found by other authors in
485 prenatal specimens (e.g. van Kampen, 1915; van der Klaauw, 1922; Reinbach, 1952). In our
486 prepared skulls, we did not find cartilage but there were several ossified entotympanic
487 elements in this region, similar to what was reported by Patterson et al. (1989) and Wible
488 (2010) in *D. novemcinctus*. The middle ear cavity volume is relatively small, both middle ear
489 muscles are well-developed and, as mentioned above, a large *pars flaccida* appears to be
490 present. The malleus has a small head, large transversal lamina and a broad articulation with
491 the ectotympanic by means of the anterior process; its manubrium is almost parallel to the
492 anatomical axis. This conforms to Fleischer's 'ancestral' ossicular morphology, found in species
493 such as the opossum *Didelphis* and believed to be primitive for therian mammals. Patterson et
494 al. (1992) found a very similar malleus morphology in the tolypeutines *Priodontes*, *Cabassous*
495 and *Tolypeutes*. We agree with those authors that this is likely to have been the primitive
496 ossicular morphology for armadillos.

497 The other armadillos examined here have complete bullae, the bulla being markedly
498 extended into a bony external auditory meatus in the euphractines, and ossicles somewhere
499 between 'transitional' and 'freely mobile' types. Those of *C. vellerosus* come closest to the
500 latter based on the prominent malleus head, small transversal lamina and the angle between
501 manubrium and anatomical axis most nearly approaching 90 degrees. These we interpret as
502 derived characteristics for armadillos. Fleischer described freely mobile mallei as having
503 abbreviated anterior processes, connected to the skull only through ligaments. This would
504 contribute to a higher acoustic compliance, promoting low-frequency sound transmission.
505 However, in many mammals usually regarded as having 'freely mobile' ossicles, the anterior
506 process actually retains a bony connection with the skull at its tip (Mason, 2006, 2016b; Mason
507 et al., 2018). The bone of the anterior process tends to be very thin, and the articulation is
508 flexible in fresh specimens. Armadillos represent a curious case in this respect: all retain very

long anterior processes, the distal halves of which articulate with the ectotympanic bone. However, there is no synostosis except, in some species (*C. truncatus*, *C. vellerosus* and *Z. pichiy*), at the very tip of the process. Whether the narrow, proximal part of the anterior process retains sufficient flexibility for armadillos to be regarded as functionally 'freely mobile' remains to be tested experimentally.

Billet et al. (2015) performed a detailed morphological study of the bony labyrinth of 17 extant xenarthran species, showing among other things that *C. truncatus*, *C. vellerosus*, *Z. pichiy* and *Euphractus sexcinctus* are characterised by a large size of the fenestra vestibuli (oval window). This, they suggested, might be considered to be a synapomorphy supporting a placement of fairy armadillos close to euphractines. The oval window accommodates the stapes footplate, quite snugly in all armadillos in contrast to some subterranean rodents (Mason et al., 2010, 2016). Its relatively large size in *Chlamyphorus* and euphractines could be associated with their movement away from the ancestral ear morphology as found in *Dasypus*, which has a very small stapes footplate. This might have occurred convergently in the chlamyphorines and euphractines. Although the ossicles of both groups are similar, those of *Chlamyphorus* appear to be more flimsily constructed: the malleus head is small and excavated, the manubrium is thin and lacks a prominent lateral process and the stapes footplate has a very thin neck and a poorly-developed labrum.

The malleo-incudal articulation

Flattened malleo-incudal articulations have been reported in many fossorial mammals (Segall, 1973; Burda et al. 1992). This may be linked to the fact that variations in static air pressure in the external ear canal cause translational (inward-outward) movements of the malleus (Hüttenbrink, 1988): the flattened articulation in subterranean mammals might help their ossicles to accommodate to air pressure changes experienced underground (Mason, 2006). Segall (1976) reported that *C. truncatus* has a malleo-incudal joint intermediate between those

of more exclusively subterranean and non-fossorial species. We found it to be more flattened than in the other armadillos studied here.

The incudo-stapedial articulation

In most mammals, the incudo-stapedial articulation involves a lenticular apophysis: a disc-like, bony process, connected to the end of the long process of the incus by means of a thin pedicle. Its medial face represents the facet for articulation with the stapes. Surprisingly, we found no pedicellate lenticular apophysis in any armadillo specimen. It was clear from our scans and reconstructions that the stapes instead articulates directly with the flattened, spatulate end of the incudal long process. We suspect that previous descriptions of a lenticular apophysis in armadillos (Fleischer, 1973; Sidorkewicj & Casanave, 2012) were based either on interpreting the flattened articulation facet on the long process of the incus as the apophysis, or on specimens in which the stapes head had broken from the stapes body and remained in articulation with the incus. The lack of a pedicellate lenticular apophysis is highly unusual among mammals but has previously been documented in monotremes, cetaceans and sirenians (Fleischer, 1973, 1978).

The thin pedicle connecting the lenticular apophysis to the long process of the incus in most mammals is predicted to confer significant flexibility (Funnell et al. 2005). Especially long pedicles have been documented in the saltatorial rodent *Jaculus* (Mason, 2016b) and in the subterranean mole-rat *Spalax*, which communicates with conspecifics by head-thumping on its burrow walls (Mason et al. 2010). A long pedicle might help to decouple the stapes and hence the inner ear from impacts affecting the malleus and incus. A similar function in armadillos might be served by the very thin neck of the stapes, which is made of essentially laminar bone and is likely to be quite flexible when hydrated.

Middle ear cavity volume

Middle ear cavity volumes can vary greatly among mammals, even within the same family or in related groups (Lay, 1972; Webster & Webster, 1975; Mason, 2013, 2016b). Enlarged middle ear cavity volumes are expected to benefit low-frequency hearing in small mammals (reviewed by Mason, 2016b). This is because cavity compliance, which is proportional to volume, tends to dominate overall middle ear compliance in small mammals, and this limits sound transmission at low frequencies (Ravicz et al. 1992). In some subterranean species, enlarged middle ear cavities could represent an adaptation for underground vocal communication (Schleich & Vassallo, 2003). However, middle ear cavity volume is not particularly large in subterranean mammals (Mason, 2001): the largest middle ear cavity volumes relative to body size are actually found in species from arid regions, including gerbils, kangaroo rats, chinchillas and certain sengis (Lay, 1972; Webster & Webster, 1975; Mason, 2013, 2016b). This may be advantageous given that lower frequencies propagate better than higher ones in arid environments (Huang et al. 2002; Rosowski et al. 2006).

Among armadillos studied, the species with by far the largest middle ear cavity volume in both absolute and relative terms was *C. vellerosus* (Table 2 and Fig. 7A). Its capacious middle ear is based in part on the great dorsal expansion of the epitympanic recess, as well as the presence of a mastoid cavity. The tympanic cavity proper is also large (note that absolute values are similar to those of *C. villosus*, Table 2).

Petter (1953) measured bullar length in gerbils and presented this as a percentage of skull length, in order to compare relative sizes between species. In their studies on armadillos, Roig (1972) and Squarcia et al. (2007) referred to this percentage value as the 'bullar hypertrophy index' (BHI). Roig established three well-defined groups based on BHI, and related the degree of hypertrophy of the species with the aridity of the environment they inhabit. Groups were (1) species without hypertrophied bullae, which live in relatively damp environments; (2) species with moderately hypertrophied bullae, which range in their distribution from semi-

586 humid to semi-arid environments; and (3) species with more hypertrophied bullae, which are
587 typically inhabitants of semi-arid and arid environments. Roig placed *Dasypus hybridus* and *D.*
588 *novemcinctus* (mean BHI: 6.42% in both cases) within Group 1, together with *Priodontes*
589 *giganteus* (= *P. maximus*; mean BHI: 4.80%), a typical inhabitant of warm and humid regions,
590 and a species referred to as '*Cabassous loricatus*' (mean BHI: 9.09%), the identity of which is
591 unclear. Group 2 included only *Tolypeutes matacus* and *Euphractus sexcinctus* (mean BHI:
592 10.47% and 12.59%, respectively), whereas Group 3 encompassed *Chaetophractus*, *Zaedyus*
593 and *Chlamyphorus* species. The largest BHI found by Roig was that of *C. vellerosus* (17.28%).
594 Similar results were reported by Squarcia et al. (2007) for *Chaetophractus* and *Zaedyus* species.
595 Our reconstructions allowed us to measure the actual middle ear cavity volumes, which are
596 affected not just by external bullar dimensions but also by expansions of the cavities into the
597 surrounding bones of the skull. We found that among the species we studied, *C. vellerosus* has
598 the largest middle ear cavity volume while *D. hybridus* has the smallest, relative to skull size
599 (Fig. 7).

600 Although some degree of overlap in the distribution of the species occurs within central
601 Argentina, *D. hybridus* appears to be more influenced by levels of precipitation than are the
602 other armadillos considered here. It is the species with highest probability of occurrence in
603 north-eastern areas of the country (Abba et al. 2012), where the mean annual precipitation
604 exceeds 1400 mm (based on climatological data from Bianchi & Cravero, 2017).
605 *Chaetophractus vellerosus*, on the other hand, is a typical inhabitant of xeric habitats from low
606 to high elevations (Wetzel et al. 2007), with high probability of occurrence in the north-west of
607 Argentina (Abba et al. 2012). Middle ear cavity expansion in *C. vellerosus* may therefore be
608 related to the aridity of its habitat, echoing Roig's (1972) conclusion. Based on its expanded
609 middle ear cavities, we predict that *C. vellerosus* has the best low-frequency hearing among
610 the species examined, but it would be premature to link this with the loud distress calls from
611 which it derives its English name, screaming hairy armadillo (Amaya et al., 2019). Within the

612 group *C. villosus* - *Z. pichiy* - *C. truncatus*, although the correlation between middle ear cavity
613 volume and aridity of habitat is less clear, their relatively large middle ear cavities and ossicular
614 structures suggest some degree of adaptation to low-frequency hearing, relative to the
615 ancestral state found in *Dasypus*. The retention of ancestral ear structures in *Dasypus* might
616 represent phylogenetic inertia rather than an adaptive fit to a specific type of environment.
617
618 *Area and lever ratios*
619 Anatomical area and lever ratios have been classically used in 'ideal transformer' models of the
620 impedance-matching function of the mammalian middle ear (e.g. Dallos, 1973). Mason (2001)
621 found that fossorial mammals tend to have lower area ratios than non-fossorials, as a result of
622 relatively large stapes footplate areas. Lever ratios also tend to be lower in fossorials although
623 malleus and incus lever arms considered individually do not differ significantly in length
624 between fossorial and non-fossorial mammals (Mason, 2001). The mean area and lever ratios
625 found here in *C. truncatus* (21.79 and 2.19, respectively) were intermediate between the mean
626 values reported by Mason for fossorial and non-fossorial mammals (area ratios: 17.11 and
627 28.27, respectively; lever ratios: 1.72 and 2.24, respectively). Although the anatomical area
628 ratio in *Chlamyphorus* was the lowest among the armadillos studied, its lever ratio was only
629 exceeded by those of both *Chaetophractus* species.
630 'Ideal transformer' models of middle ear function are subject to significant criticism based
631 on their oversimplifications, and their predictions are often not supported by experimental
632 measurements (see Mason, 2016a for a recent review). Middle ear function is greatly
633 complicated by the flexibility and frequency-dependent vibrational characteristics of the
634 tympanic membrane and ossicular chain. Therefore, although gross differences in anatomical
635 area and lever ratios among mammals can probably still tell us something about the nature of
636 their hearing, small differences such as those found among the armadillos in this study are of
637 doubtful functional significance.

Conclusion

In comparison with the middle ear apparatus of *Dasypus*, which is interpreted here as being primitive for Cingulata, the pink fairy armadillo *Chlamyphorus truncatus* shows some derived characteristics. These include the development of a complete auditory bulla which accommodates a relatively larger middle ear cavity volume, a reduced pars flaccida, ossicles which have moved towards a 'freely mobile' morphology, the reduction or loss of the tensor tympani muscle and a more flattened malleo-incudal articulation. This mirrors the direction of evolution documented among the subterranean talpid moles, in comparison with their more terrestrial relatives (Mason, 2006). However, the first three of these characteristics are shared with euphractine armadillos and so cannot necessarily be considered to represent adaptations to the more exclusively subterranean environment of *Chlamyphorus*. All of these armadillos including *Chlamyphorus* have long anterior processes and lack pedicellate lenticular apophyses, neither of which is expected of subterranean mammals. The reduction of the tensor tympani and the thin, flimsy appearance of the ossicles of *Chlamyphorus* might in fact be indicative of degeneration of the ear: in this respect there are interesting parallels with the naked mole-rat, *Heterocephalus glaber*, the small, delicate ossicles of which have also been considered potentially degenerate (Mason et al., 2016). In terms of low-frequency specialisation, it is actually *Chaetophractus vellerosus* which stands out among armadillos, based on its voluminous middle ear cavity. Given its association with xeric habitats, this can be added to the list of arid-region mammals with markedly hypertrophied middle ear cavities.

Acknowledgements

Financial support from the following sources is acknowledged: Secretaría General de Ciencia y Tecnología, UNS (Project PGI 24/B243); Consejo Nacional de Investigaciones Científicas y

Técnicas (CONICET) through a PhD fellowship to APB; Subsecretaría de Relaciones Internacionales, UNS, through a grant to APB for Postgraduate Mobility. Authors also thank Dr. Flavia Buffo (Dpto. Matemática, UNS) for her helpful assistance in algebraic procedures, and the Cambridge Biotomography Centre for the use of their scanner. Finally, thanks are due to the two anonymous reviewers of this manuscript for their helpful comments and suggestions.

Conflict of interest

The authors have no conflict of interests.

References

Abba AM, Tognelli MF, Seitz VP, et al. (2012) Distribution of extant xenarthrans (Mammalia: Xenarthra) in Argentina using species distribution models. *Mammalia* **76**, 123-136.

Aguiar JM, Fonseca GAB (2008) Conservation status of the Xenarthra. In: *The Biology of the Xenarthra* (eds Vizcaíno SF, Loughry WJ), pp. 215-231. Gainesville: University Press of Florida.

Amaya JP, Zufiaurre E, Areta JI, et al. (2019) The weeping vocalization of the screaming hairy armadillo (*Chaetophractus vellerosus*), a distress call. *J Mammal* gyz108. http://doi.org./10.1093/jmammal/gyz108. 9pp.

Argyle EC, Mason MJ (2008) Middle ear structures of *Octodon degus* (Rodentia: Octodontidae), in comparison with those of subterranean caviomorphs. *J Mammal* **89**, 1447-1455.

Begall S, Burda H (2006) Acoustic communication and burrow acoustics are reflected in the ear morphology of the coruro (*Spalacopus cyanus*, Octodontidae), a social fossorial rodent. *J Morphol* **267**, 382-390.

687 **Begall S, Lange S, Schleich CE, et al.** (2007) Acoustics, Audition and Auditory System. In:
688 *Subterranean Rodents: News from Underground* (eds Begall S, Burda H, Schleich CE), pp.
689 97-111. Berlin Heidelberg: Springer-Verlag.

690 **Bianchi AR, Cravero SAC (2017)** Atlas climático digital de la República Argentina. INTA
691 (Instituto Nacional de Tecnología Agropecuaria).
692 http://geoportal.idesa.gob.ar/layers/geonode%3Aprecipitacion_anual.

693 **Billet G, Hautier L, Lebrun R.** (2015) Morphological diversity of the bony labyrinth (inner ear) in
694 extant xenarthrans and its relation to phylogeny. *J Mammal* **96**, 658-672.

695 **Borghi CE, Giannoni SM, Roig VG** (2002) Eye reduction in subterranean mammals and eye
696 protective behavior in *Ctenomys*. *J Neotrop Mammal* **9**, 123-134.

697 **Borghi CE, Campos CM, Giannoni SM, et al.** (2011) Updated distribution of the pink fairy
698 armadillo *Chlamyphorus truncatus* (Xenarthra, Dasypodidae), the world's smallest
699 armadillo. *Edentata* **12**, 14-19.

700 **Burda H, Bruns V, Hickman GC** (1992) The ear in subterranean Insectivora and Rodentia in
701 comparison with ground-dwelling representatives. I. Sound conducting system of the
702 middle ear. *J Morphol* **214**, 49-61.

703 **Burda H, Bruns V, Nevo E** (1989) Middle ear and cochlear receptors in the subterranean mole-
704 rat*, Spalax ehrenbergi*. *Hear Res* **39**, 225-230.

705 **Brückmann G, Burda H** (1997) Hearing in blind subterranean Zambian mole-rats (*Cryptomys*
706 sp.): collective behavioural audiogram in a highly social rodent. *J Comp Physiol A* **181**, 83-88.

707 **Casanave EB, Galíndez EJ** (2008) The spleen of the armadillo. Lessons of organ adaptation. In:
708 *The Biology of the Xenarthra* (eds Vizcaíno SF, Loughry WJ), pp. 120-125. Gainesville:
709 University Press of Florida.

710 **Dallos P** (1973) *The auditory Periphery. Biophysics and Physiology*. New York: Academic Press.

711 **Delsuc F, Superina M, Tilak M-K, et al.** (2012) Molecular phylogenetics unveils the ancient
712 evolutionary origins of the enigmatic fairy armadillos. *Mol Phylogenet Evol* **62**, 673-680.

713 **Doran AHG** (1878) Morphology of the mammalian Ossicula auditûs. *Trans Linn Soc Lond (Zool)*
714 **1**, 371-504.

715 **Fleischer G** (1973) Studien am Skelett des Gehörorgans der Säugetiere, einschlieβlich des
716 Menschen. *Säugetierkd Mitt* **21**, 131-239.

717 **Fleischer G** (1978) Evolutionary principles of the mammalian middle ear. *Adv Anat Embryol Cell*
718 *Biol* **55**, 1-70.

719 **Funnell WRJ, Siah TH, McKee MD, et al.** (2005) On the coupling between the incus and the
720 stapes in the cat. *J Assoc Res Oto* **6**, 9-18.

721 **Galliari FC** (2014) El tipo *scratch-digger* en dos armadillos (Dasypodidae, Xenarthra): ontogenia
722 esqueletaria de las manos y variaciones de dígitos. *Rev Museo La Plata, Sección Zool* **24**, 1-
723 14.

724 **Gerhardt P, Henning Y, Begall S, et al.** (2017) Audiograms of three subterranean rodent
725 species (genus *Fukomys*) determined by auditory brainstem responses reveal extremely
726 poor high-frequency hearing. *J Exp Biol* **220**, 4377-4382.

727 **Gibb GC, Condamine FL, Kuch M, et al.** (2016) Shotgun mitogenomics provides a reference
728 phylogenetic framework and timescale for living xenarthrans. *Mol Biol Evol* **33**, 621-642.

729 **Graboyes EM, Chole RA, Hullar TE** (2011) History of Otology. The Ossicle of Paaw. *Otol*
730 *Neurotol* **32**, 1185-1188.

731 **Heffner RS, Heffner HE** (1990) Vestigial hearing in a fossorial mammal, the pocket gopher
732 (*Geomys bursarius*). *Hear Res* **46**, 239-252.

733 **Heffner RS, Heffner HE** (1992) Hearing and sound localization in blind mole rats (*Spalax*
734 *ehrenbergi*). *Hear Res* **62**, 206-216.

Heffner RS, Heffner HE (1993) Degenerate hearing and sound localization in naked mole rats (*Heterocephalus glaber*), with an overview of central auditory structures. *J Comp Neurol* **331**, 418-433.

Henson O'DW Jr. (1961) Some morphological and functional aspects of certain structures of the middle ear in bats and insectivores. *Univ Kans Sci Bull* **42**, 151-249.

Heth G, Frankenberg E, Nevo E (1986) Adaptive optimal sound for vocal communication in tunnels of a subterranean mammal (*Spalax ehrenbergi*). *Experientia* **42**, 1287-1289.

Hinchclifee R, Pye A (1969) Variations in the middle ear of the Mammalia. *J Zool (Lond)* **157**, 277-288.

Huang GT, Rosowski JJ, Ravicz ME, et al. (2002) Mammalian ear specializations in arid habitats: structural and functional evidence from sand cat (*Felis margarita*). *J Comp Physiol A* **188**, 663-681.

Hüttenbrink KB (1988) The Mechanics of the middle-ear at static air pressures: The role of the ossicular joints, the function of the middle-ear muscles and the behaviour of stapedial prostheses. *Acta Otolaryngol* **451 (Suppl)**, 1-35.

Hyrtl J (1845) *Vergleichend-anatomische Untersuchungen über das innere Gehörorgan des Menschen und der Säugethiere*. Verlag von Friedrich Ehrlich, Prague.

Lange S, Stalleicken J, Burda H. (2004) Functional morphology of the ear in fossorial rodents, *Microtus arvalis* and *Arvicola terrestris*. *J Morphol* **262**, 770-779.

Lavender D, Taraskin SN, Mason MJ (2011) Mass distribution and rotational inertia of "microtype" and "freely mobile" middle ear ossicles in rodents. *Hear Res* **282**, 97-107.

Lay DM (1972) The anatomy, physiology, functional significance and evolution of specialized hearing organs of gerbilline rodents. *J Morph* **138**, 41-120.

Loughry WJ, Prodöhl PA, McDonough CM, et al. (1998) Polyembryony in armadillos. *Am Sci* **86**, 274-279.

Madsen O, Scally M, Douady CJ, et al. (2001) Parallel adaptive radiations in two major clades of placental mammals. *Nature* **409**, 610-614.

Mason MJ (2001) Middle ear structures in fossorial mammals: a comparison with non-fossorial species. *J Zool (Lond)* **255**, 467-486.

Mason MJ (2003) Morphology of the middle ear of golden moles (Chrysochloridae). *J Zool (Lond)* **260**, 391-403.

Mason MJ (2004) The middle ear apparatus of the tuco-tuco *Ctenomys sociabilis* (Rodentia, Ctenomyidae). *J Mammal* **85**, 797-805.

Mason MJ (2006) Evolution of the middle ear apparatus in talpid moles. *J Morph* **267**, 678–695.

Mason MJ (2013) Of mice, moles and guinea pigs: Functional morphology of the middle ear in living mammals. *Hear Res* **301**, 4-18.

Mason MJ (2015) Functional morphology of rodent middle ears. In: *Evolution of the Rodents: Advances in Phylogeny, Functional Morphology and Development* (eds Cox PG, Hautier L), pp. 373-404. Cambridge: Cambridge University Press.

Mason MJ (2016a) Structure and function of the mammalian middle ear. II: Inferring function from structure. *J Anat* **228**, 300-312.

Mason MJ (2016b) Structure and function of the mammalian middle ear. I: Large middle ears in small desert mammals. *J Anat* **228**, 284-299.

Mason MJ, Bennett NC, Pickford M (2018) The middle and inner ears of the Palaeogene golden mole *Namachloris*: A comparison with extant species. *J Morphol* **00**, 1-21. https://doi.org/10.1002/jmor.20779.

782 **Mason MJ, Cornwall HL, Smith ESJ** (2016) Ear structures of the naked mole-rat,
783 *Heterocephalus glaber* , and its relatives (Rodentia: Bathyergidae). *PLoS ONE* **11**, e0167079.

784 **Mason MJ, Lai FWS, Li JG, et al.** (2010) Middle ear structure and bone conduction in *Spalax*,
785 *Eospalax*, and *Tachyoryctes* mole-rats (Rodentia: Spalacidae). *J Morphol* **271**, 462-472.

786 **McClain JA** (1939) The development of the auditory ossicles of the opossum (*Didelphys*
787 *virginiana*). *J Morphol* **64**, 211-265.

788 **McDonald HG** (2005) Paleoecology of extinct xenarthrans and the Great American Biotic
789 Interchange. *Bull Fla Mus Nat Hist* **45**, 313-333.

790 **McNab BK** (1980) Energetics and the limits to a temperate distribution in armadillos. *J*
791 *Mammal* **61**, 606-627.

792 **Meritt Jr DA** (1985) The fairy armadillo, *Chlamyphorus truncatus* Harlan. In: *The Evolution and*
793 *Ecology of Armadillos, Sloths, and Vermilinguas* (ed. Montgomery GC), pp. 393-395.
794 Washington and London: Smithsonian Institution Press.

795 **Milne N, Vizcaíno SF, Fernicola JC** (2009) A 3D geometric morphometric analysis of digging
796 ability in the extant and fossil cingulate humerus. *J Zool* **278**, 48-56.

797 **Minoprio JDL** (1945) Sobre el *Chlamyphorus truncatus* Harlan. *Acta Zool Lilloana* **3**, 5-58.

798 **Murphy WJ, Eizirik E, Johnson WE, et al.** (2001) Molecular phylogenetics and the origins of
799 placental mammals. *Nature* **409**, 614-618.

800 **Novacek MJ (1977)** Aspects of the problem of variation, origin and evolution of the eutherian
801 auditory bulla. *Mammal Rev* **7**, 131-149.

802 **Novacek MJ, Wyss A** (1986) Origin and transformation of the mammalian stapes. In:
803 *Vertebrates, Phylogeny, and Philosophy* (eds Flanagan KM, Lillegraven JA), pp. 35-53.
804 Contributions to Geology, University of Wyoming, Special Paper 3.

Ojeda RA, Chillo V, Díaz G (2012) *Libro Rojo de Mamíferos Amenazados de la Argentina*. Sociedad Argentina para el Estudio de los Mamíferos (SAREM).

Paaw P (1615) *Primitiae Anatomicae. De Humani Corporis Ossibus*. The Netherlands: Lugduni Batauorum, ex officina Ivsti à Colster.

Patterson B, Segall W, Turnbull WD (1989) The ear region in xenarthrans (= Edentata: Mammalia). Part I. Cingulates. *Fieldiana: Geology (NS)* **18**, 1-46.

Patterson B, Segall W, Turnbull WD, et al. (1992) The ear region in xenarthrans (= Edentata: Mammalia). Part II. Pilosa (sloths, anteaters), palaeanodonts, and a miscellany. *Fieldiana: Geology (NS)* **24**, 1-79.

Petter F (1953) Remarques sur la signification des bulles tympaniques chez les mammifères. *C R Hebd Séances Acad Sci* **237**, 848-849.

Pye A (1972) Variations in the structure of the ear in the different mammalian species. *British J Audiol* **6**, 14-18.

Ravicz ME, Rosowski JD, Voigt HF (1992) Sound-power collection by the auditory periphery of the Mongolian gerbil Meriones unguiculatus. I: Middle-ear input impedance. *J Acoust Soc Am* **92**, 155-177.

Reinbach VW (1952) Zur Entwicklung des Primordialcraniums von *Dasypus novemcinctus* Linné (*Tatusia novemcincta* Lesson) I. *Z Morph Anthropol* **44**, 375-444.

Roig VG (1972) La hipertrofia de la bula timpánica y su significado adaptativo en los edentados de zonas áridas. *Deserta* **2**, 87-97.

Rood JP (1970) Notes on the behavior of the pygmy armadillo. *J Mammal* **51**, 179.

Rosowski JJ, Ravicz ME, Songer JE (2006) Structures that contribute to middle-ear admittance in chinchilla. *J Comp Physiol A* **192**, 1287-1311.

Schleich CE, Vassallo AI (2003) Bullar volume in subterranean and surface-dwelling caviomorph rodents. *J Mammal* **84**, 185-189.

Segall W (1973) Characteristics of the ear, especially the middle ear in fossorial mammals, compared with those in the Manidae. *Acta Anat* **86**, 96-110.

Segall W (1976) Further observations on the ear in fossorial mammals with special considerations of *Chlamyphorus truncatus* (Harlan). *Acta Anat* **94**, 431-444.

Sidorkewicj NS, Casanave EB (2012) Morphology of the middle ear in three species of armadillos (Dasypodidae, Xenarthra) from Argentina. *Int J Morphol* **30**, 1500-1507.

Sidorkewicj NS, Casanave EB (2013) Morphological characterization and sex-related differences of the mandible of the armadillos *Chaetophractus vellerosus* and *Zaedyus pichiy* (Xenarthra, Dasypodidae), with consideration of dietary aspects. *Iheringia, Sér Zool* **103**, 153-162.

Squarcia SM, Sidorkewicj NS, Casanave EB (2007) The hypertrophy of the tympanic bulla in three species of dasypodids (Mammalia, Xenarthra) from Argentina. *Int J Morphol* **25**, 597-602.

Superina M (2006) New information on population declines in pink fairy armadillos. *Edentata* **7**, 48-50.

Superina M, Abba AM, Roig VG (2014) *Chlamyphorus truncatus*. The IUCN Red List of Threatened Species 2014: e.T4704A47439264. http://dx.doi.org/10.2305/IUCN.UK.2014-1.RLTS.T4704A47439264.en. Downloaded on 01 June 2019.

Tarver JE, dos Reis M, Mirarab S, et al. (2016) The interrelationships of placental mammals and the limits of phylogenetic inference. *Genome Biol Evol* **8**, 330-344.

Torres R, Abba AM, Superina M (2015) Climate fluctuations as a cause of rarity in fairy armadillos. *Mammal Biol* **80**, 452-458.

852 **van Kampen PN** (1915) De phylogenie van het entotympanicum. *Tijdschr Ned Dierkd Ver* **14**,
853 XXIV.

854 **van der Klaauw CJ** (1922) Über die Entwickelung des Entotympanicums. *Tijdschr Ned Dierkd*
855 *Ver* **18**, 135-174.

856 **Vizcaíno SF, Fariña RA, Mazzetta GV** (1999) Ulnar dimensions and fossoriality in armadillos
857 and other South American mammals. *Acta Theriol* **44**, 309-320.

858 **Webster DB, Webster M** (1975) Auditory systems of Heteromyidae: postnatal development of
859 the ear of *Dipodomys merriami*. *J Morphol* **146**, 377-393.

860 **Wetzel RM, Gardner AL, Redford KH, et al.** (2007) Order Cingulata. In: *Mammals of South*
861 *America, Volume 1: Marsupials, Xenarthrans, Shrews and Bats* (ed. Gardner AL), pp. 128-
862 157. Chicago: The University of Chicago Press, Chicago.

863 **Wible JR** (2009) The ear region of the pen-tailed treeshrew, *Ptilocercus lowii* Gray, 1848
864 (Placentalia, Scandentia, Ptilocercidae). *J Mammal Evol* **16**, 199-233.

865 **Wible JR** (2010) Petrosal Anatomy of the Nine-Banded Armadillo, *Dasypus novemcinctus*
866 Linnaeus, 1758 (Mammalia, Xenarthra, Dasypodidae). *Ann Carnegie Mus* **79**, 1-28.

867

868 **Table 1** Details of specimens used in this study with indication of sex, total skull length (TSL)
869 and what was scanned (E: isolated temporal bone/ear region; P: posterior skull; S: whole skull).
870 Body masses of adults (mixed sexes) of comparable skull sizes and coming from the same
871 geographical area are given (mean ± standard deviation), with an indication of the sample size
872 (n) with which that information was obtained (data from Sidorkewicj, Basso & Casanave,
873 unpublished).
874

Family (Subfamily)	Species	Specimen code	Body mass (g)	Sex	TSL (mm)	Scanned
Chlamyphoridae (Chlamyphorinae)	*Chlamyphorus truncatus*	UNSCTMA1	99 ± 5 (n=4)	Male	39.34	P
		UNSCTSI1		Unknown	36.12	P
		UNSCTSI2		Unknown	36.61	S
Chlamyphoridae (Euphractinae)	*Chaetophractus villosus*	UNSCVIMA87	3285 ± 726 (n=21)	Male	94.49	E
		UNSCVIMA91		Male	92.25	E
		UNSCVIHA83		Female	94.57	P, S
		UNSCVIHA89		Female	93.70	E
	Chaetophractus vellerosus	UNSCVEHA80	1040 ± 135 (n=11)	Female	69.02	E, P, S
	Zaedyus pichiy	UNSZPMA52	986 ± 186 (n=13)	Male	64.42	S
		UNSZPHA55		Female	65.48	E, S
		UNSZPSI4		Unknown	66.03	P
Dasypodidae (Dasypodinae)	*Dasypus hybridus*	UNSDHHA2	1775 ± 456 (n=8)	Female	72.77	S
		UNSDHHA4		Female	76.13	P

875
876
877

878 **Table 2** Total volumes of the middle ear cavity (MEC) and of its subcavities (TC: tympanic
879 cavity; ER: epitympanic recess; MC: mastoid cavity), obtained from CT reconstructions. TSL:
880 total skull length (mm). For *Chlamyphorus truncatus*, *Chaetophractus villosus* and *Zaedyus*
881 *pichiy*, mean values (± standard deviation) are presented.
882

Species	TSL (mm)	MEC volume (mm^3)	TC volume (mm^3)	ER volume (mm^3)	MC volume (mm^3)
Chlamyphorus truncatus (n=2)	37.73 ± 2.28	38.64 ± 3.46	33.44 ± 3.27	5.20 ± 0.20	---
Chaetophractus villosus (n=4)	93.75 ± 1.08	497.87 ± 71.61	407.22 ± 69.60	90.65 ± 15.58	---
Chaetophractus vellerosus (n=1)	69.02	821.02	409.56	337.22	74.24
Zaedyus pichiy (n=3)	65.31 ± 0.82	193.78 ± 6.97	155.11 ± 9.67	38.67 ± 11.27	---
Dasypus hybridus (n=1)	76.13	35.07	28.68	6.39	---

883
884
885
886

887 **Table 3** Measurements made from the middle ear reconstructions in armadillos.

888

Species	Malleus volume (mm^3)	Incus volume (mm^3)	Stapes volume (mm^3)	Tympanic membrane *pars tensa* area (mm^2)	Stapes footplate area (mm^2)	Area ratio	Malleus lever arm (mm)	Incus lever arm (mm)	Lever ratio
Chlamyphorus truncatus (n=2)	0.42 ± 0.03	0.29 ± 0.01	0.05 ± 0.01	11.32 ± 0.40	0.52 ± 0.01	21.79 ± 1.35	2.62 ±0.07	1.20 ± 0.01	2.19 ± 0.05
Chaetophractus villosus (n=4, except where specified)	5.78 ± 0.30	4.45 ± 0.37	0.18 ± 0.02 (n=2)	56.39 ± 4.22	1.15 ± 0.05	49.29 ± 3.68	5.37 ± 0.48 (n=2)	2.33 ± 0.24 (n=2)	2.31 ± 0.03 (n=2)
Chaetophractus vellerosus (n=1)	4.43	3.47	0.20	44.33	1.37	32.36	5.19	1.84	2.82
Zaedyus pichiy (n=3)	2.65 ± 0.23	1.80 ± 0.18	0.18 ± 0.07	29.92 ± 0.82	0.85 ± 0.13	35.78 ± 4.44	3.77 ± 0.29	1.80 ± 0.04	2.09 ± 0.19
Dasypus hybridus (n=1)	1.12	0.41	0.05	10.17	0.34	29.91	2.25	1.12	2.01

889

890 **Table 4** Least-squares linear regression relationships between middle ear parameters (*y*) and
891 total skull length (*x*) in armadillos. Analyses were performed on log-transformed data for both
892 dependent and independent variables. The probability value of the slope coefficient *b* is
893 indicated as *p* (Regression), and the coefficient of determination as R^2; SE(*b*) represents the
894 standard error of *b*; the probability value obtained when testing the deviation of *b* from the
895 theoretical value of isometric growth is indicated as *p* (Allometry). See text for further details.

Parameter (*y*)	n	Intercept (*a*)	Slope (*b*)	*p* (Regression)	R^2	SE(*b*)	*p* (Allometry)
Middle ear cavity volume (mm^3)	11	-2.47	2.60	0.009	0.55	0.779	0.618
Malleus + incus volume (mm^3)	11	-4.47	2.77	< 0.001	0.79	0.475	0.635
Stapes volume (mm^3)	9	-3.43	1.37	0.057	0.43	0.603	0.030
Tympanic membrane (*pars tensa*) area (mm^2)	11	-1.53	1.64	0.004	0.63	0.421	0.409
Stapes footplate area (mm^2)	11	-1.48	0.76	0.060	0.34	0.355	0.007
Malleus lever arm (mm)	9	-0.62	0.65	0.055	0.43	0.284	0.261
Incus lever arm (mm)	9	-0.89	0.61	0.026	0.538	0.217	0.118

896

Appendix S1: Details of the scans made in the present study.

Species	Specimen code	Scan	mV	µA	Voxel size, micrometres
Chlamyphorus truncatus	UNSCTMA1	Posterior skull	125	120	15.5
	UNSCTSI1	Posterior skull	125	130	14.1
	UNSCTSI2	Whole skull	125	130	20.4
Chaetophractus villosus	UNSCVIMA87	Temporal bone-closed up	130	120	15.8
		Temporal bone uncropped	125	130	25.8
	UNSCVIMA91	Temporal bone	130	120	20.5
	UNSCVIHA83	Posterior skull	125	130	32.7
		Whole skull	125	130	50.9
	UNSCVIHA89	Temporal bone-closed up	130	120	18.8
Chaetophractus vellerosus	UNSCVEHA80	Posterior skull	125	130	23.9
		Temporal bone	130	120	15.4
		Whole skull	125	130	38.2
Zaedyus pichiy	UNSZPMA52	Whole skull	125	130	35.1
	UNSZPHA55	Temporal bone	130	120	13.8
		Whole skull	125	130	35.5
	UNSZPSI4	Posterior skull	125	120	23.3

Dasypus hybridus	UNSDHHA2	Whole skull	125	130	38.6
	UNSDHHA4	Posterior skull	125	130	18.5

2

3

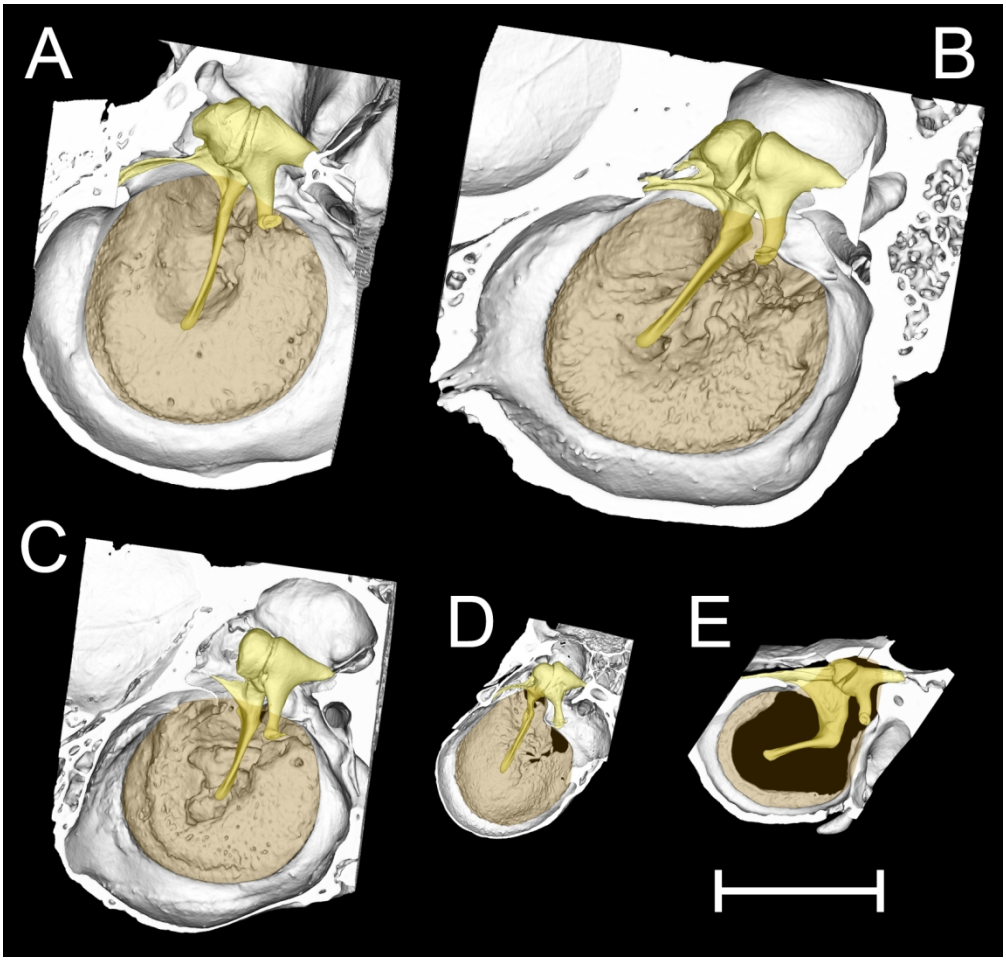

Fig. 2 3D reconstructions of the right tympanic ring, malleus and incus in five species of armadillos, from approximately medial views. Positions of the tympanic membranes are indicated by light brown shading. A: *Chaetophractus vellerosus* (UNSCVEHA80); B: *C. villosus* (UNSCVIMA87); C: *Zaedyus pichiy* (UNSZPHA55); D: *Chlamyphorus truncatus* (UNSCTSI1); E: *Dasypus hybridus* (UNSDHHA4). The scale bar represents 5 mm.

593x565mm (72 x 72 DPI)

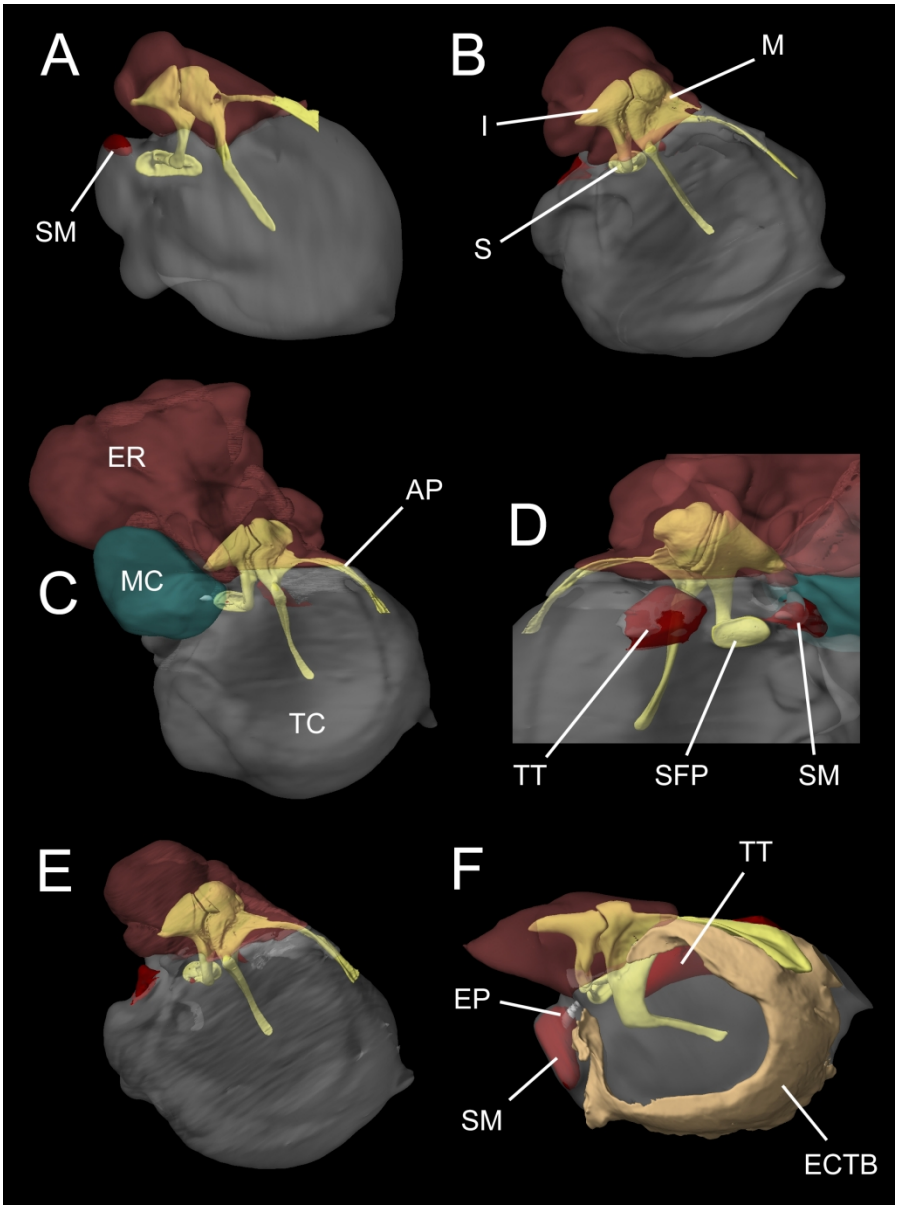

Fig. 4 Stradwin reconstructions of right middle ear structures seen from roughly lateral views. A: *Chlamyphorus truncatus* (UNSCTMA1); B: *Chaetophractus villosus* (UNSCVIMA87); C: *C. vellerosus* (UNSCVEHA80); D: detail of the middle ear ossicles and associated tissues in *C. vellerosus*, from a medial view; E: *Zaedyus pichiy* (UNSZPHA55); F: *Dasypus hybridus* (UNSDHHA4). The walls of the cavities are shown semitranslucent to reveal the internal structures. The ectotympanic bone is shown only in *D. hybridus*. Not to scale. AP, anterior process; ECTB, ectotympanic bone; EP, element of Paaw; ER, epitympanic recess; I, incus; M, malleus; MC, mastoid cavity; S, stapes; SFP, stapes footplate; SM, stapedius muscle; TC, tympanic cavity; TT, tensor tympani muscle.

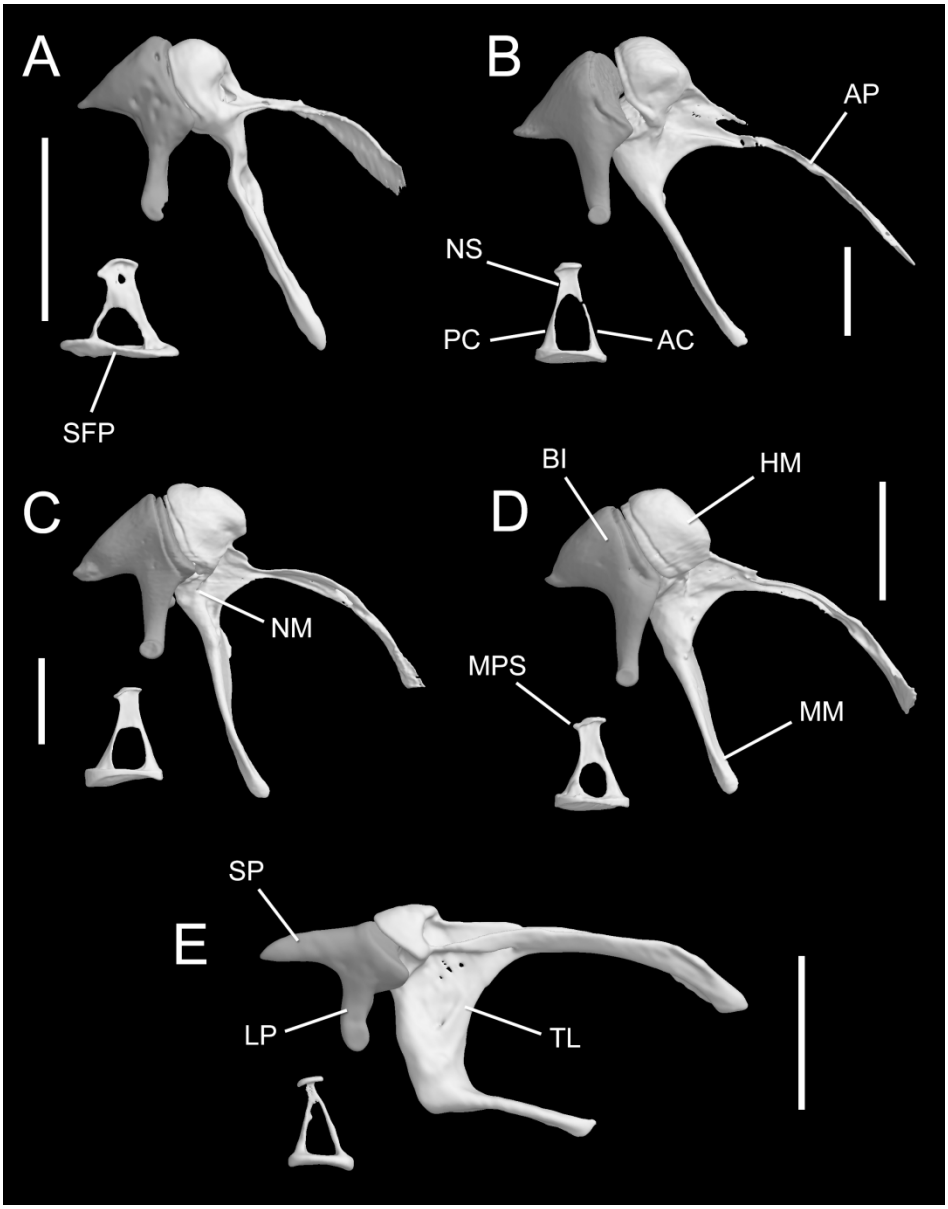

Fig. 5 Stradwin reconstructions of left middle ear ossicles of armadillos (articulated malleus and incus in approximately medial view; stapes in dorsal view). A: *Chlamyphorus truncatus* (UNSCTSI1); B: *Chaetophractus villosus* (UNSCVIMA87); C: *C. vellerosus* (UNSCVEHA80); D: *Zaedyus pichiy* (UNSZPHA55); E: *Dasypus hybridus* (UNSDHHA4). The scale bars represent 2 mm. AC, anterior crus of stapes; AP, anterior process of malleus; BI, body of incus; HM, head of malleus; LP, long process of incus; MM, manubrium of malleus; MPS, muscular process of stapes; NM, neck of malleus; NS, neck of stapes; PC, posterior crus of stapes; SFP, stapes footplate; SP, short process of incus; TL, transversal lamina of malleus.

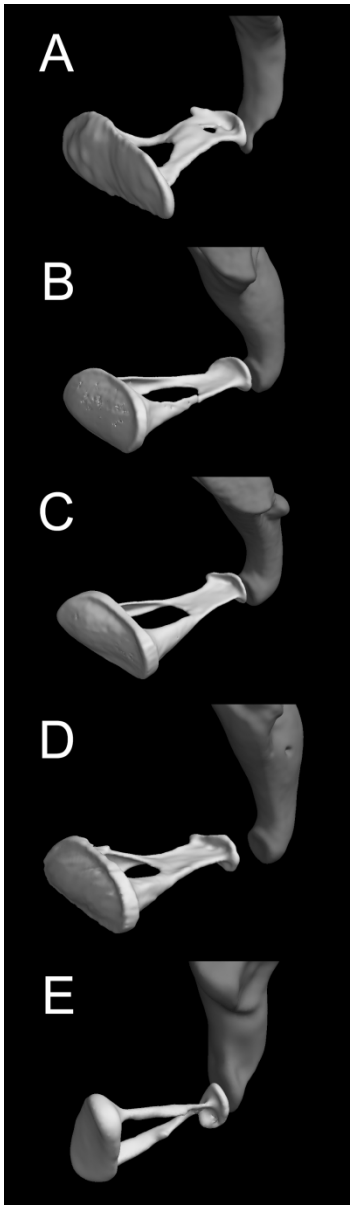

Fig. 6 Stradwin reconstructions of the left incudo-stapedial joints of armadillos, seen from rostromedially. A: *Chlamyphorus truncatus* (specimen UNSCTSI1); B: *Chaetophractus villosus* (UNSCVIMA87); C: *C. vellerosus* (UNSCVEHA80); D: *Zaedyus pichiy* (UNSZPMA55: the stapes has become disarticulated from the incus in this specimen); E: *Dasypus hybridus* (UNSDHHA4). Only the distal end of the long process of the incus and the stapes are shown. Not to scale.

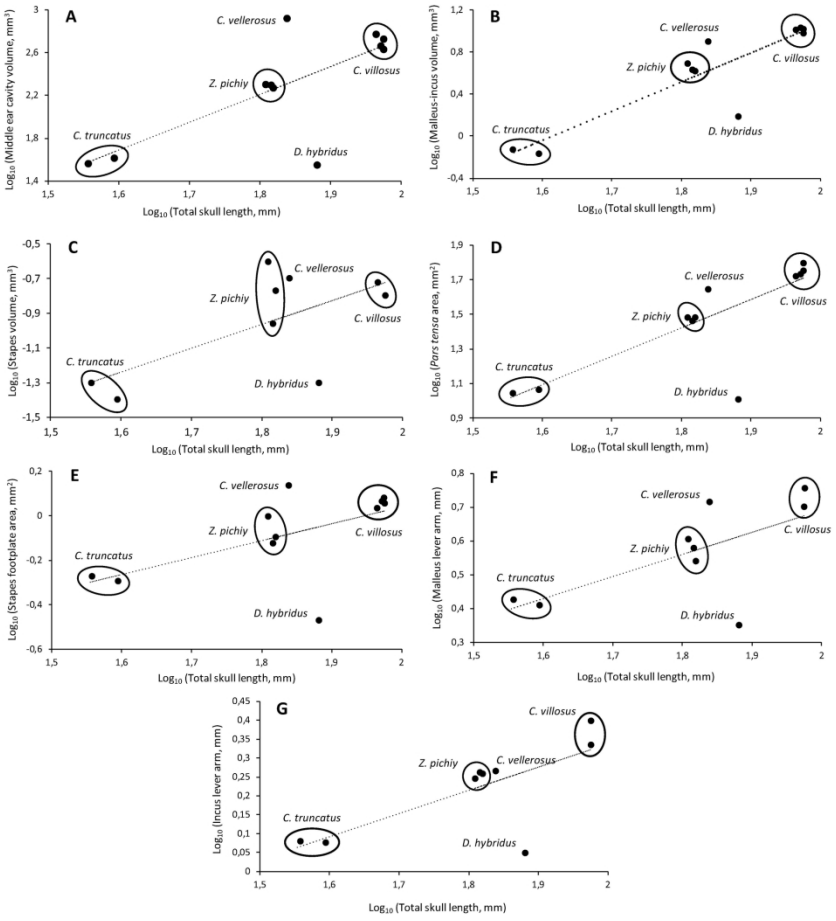

Fig. 7 Relationships between middle ear parameters and skull size in armadillos, based on log-transformed data. A: Middle ear cavity volume vs. total skull length; B: Volume of the malleo-incudal complex vs. total skull length; C: Stapes volume vs. total skull length; D: Tympanic membrane *pars tensa* area vs. total skull length; E: Stapes footplate area vs. total skull length; F: Malleus lever arm vs. total skull length; G: Incus lever arm vs. total skull length. The calculated regression lines are indicated as dotted lines. Members of the same species are ringed. See Table 4 for further information.

209x207mm (300 x 300 DPI)